`SVU International Journal of Engineering Sciences and Applications (2024) 5(2): 62-85
Print ISSN 2785-9967| Online ISSN 2735-4571
DOI 10.21608/SVUSRC.2024.250110.1162

Techno-economic Analysis of Hybrid Renewable Energy Systems Considering Demand Side Management

Reem Abdelkareem [1,*], Abdel-Raheem Youssef[1], and Mohamed A.Ismeil[1, 2]

Abstract This paper presents a study on the design of rural energy systems and provides an analysis of the technical and economic feasibility of proposed Hybrid Energy Systems (HES) for rural electrification in a village in Egypt. The Hybrid Renewable Energy Systems are designed using the standard software tool HOMER Pro, addressing the optimization challenge of designing a hybrid renewable energy system based on demand-side management during peak and off-peak hours. In this study, realistic electricity consumption data for a single-family residence is evaluated in Qena City and Red Sea City in the Arab Republic of Egypt. To evaluate the effectiveness of the recommended design plan, this study considers three different cases. Simulation results reveal that the suggested design scheme is more suitable for remote locations than the previously proposed systems, as represented in these cases. Within each city, three scenarios are examined, and the optimal combination with the lowest cost is selected. Furthermore, in unregulated energy systems in remote areas, demand-side management (DSM) proves effective in addressing uncertainties in renewable energy generation and loading.

Keywords: PV, wind, hybrid energy system, HOMER, DSM, COE, NPC.

1 Introduction

Due to the increasing demand to provide energy to remote areas where access to electricity generated by electricity networks is difficult, the use of renewable energy becomes the ideal solution to this problem. To meet the community's energy needs in remote areas, renewable energy resources are used [1]. With such a system, it would be possible to advance toward sustainable development and give all people access to reliable, affordable, clean, and secure energy. Around 1.3 billion people do not have access to electricity today, mostly in developing nations and rural areas [2]. Energy security is the equitable provision of consumers with energy services that are readily available, reasonably priced, dependable, efficient, environmentally friendly, and socially acceptable [3]. In 2021, renewable energy sources accounted for 28.7% of global electricity generation, not including hydroelectric power. Consequently, within the Indian context, a viable off-grid energy solution might involve the integration of a hybrid renewable energy system (HRES), combining energy storage with a biogas generator at a reduced cost [4]. Hybrid power supply systems provide cost-effectiveness, efficiency and reliability when compared to single-source power systems [5]. For instance, solar power generation can vary significantly in output based on the prevailing solar radiation source [6], this gives rise to concerns regarding the power generation's reliability, particularly when it's connected to the grid system. In such a scenario, solar electricity may be perceived as a liability for the grid, as it exhibits characteristics associated with uncontrollable energy sources [7]. Renewable Energy Sources offer numerous technical, financial, and environmental advantages. However, their intermittent nature poses challenges in accurately predicting electricity generation, thereby diminishing system reliability [8]. These issues can be addressed by integrating RES with other technologies or traditional energy sources to form Hybrid Renewable Energy Systems (HRES). The hybrid system's structure can be elucidated through the use of three distinct types of systems. Among these types, one may incorporate conventional systems like gas turbines, diesel generators, or even entire power plants for grid-connected hybrid systems. It is regarded as one of the constituent generating Nomenclature

Received: 20 November 2023/ Accepted: 30 January 2024
*Corresponding Author: Reem Abdelkareem, E-mail: reem882015@gmail.com
1. Electrical Engineering Department, Faculty of Engineering, South Valley University, Egypt
2.Electrical Engineering Department, Faculty of Engineering, King Khalid University, Abha 61411, Saudi Arabia.

HRES	Hybrid Renewable Energy Systems	HES	hybrid Energy Systems
DSM	Demand Side Management	CO_2	Carbon Dioxide
PSO	Particle Swam Optimization	GA	Genetic Algorithm
GPSO	Greedy Particle Swam Optimization	MODDED	Multi-Objective Dynamic Economic and Emission Dispatch
MOPSO	Multi-objective Particle Swarm Optimization	LPL	Low Priority Load
HPL	High Priority Load	CSP	concentrated solar power
GHI	global horizontal irradiance	P_{PV}	output power of the solar PV generator
N	total number of solar PV modules	A_m	total area of the PV modules
G_t	solar irradiance	η_g	PV generator's efficiency
η_{Pt}	power point tracker's efficiency	η_r	generator's reference efficiency,
T_C	PV cell's temperature	T_r	reference temperature of the PV cell
β_t	temperature coefficient of efficiency	NOCT	nominal operating cell temperature
V	wind speed	V_{in}	wind's cut-in speed
V_n	wind's rated speed	V_{out}	cutoff speed
Pm	wind turbine's rated power	P_{wt}	wind turbine power
LCOE	levelized cost of electricity	LRMC	long-run marginal cost
a_1	grid extension constant related to distance	a_2	grid extension constant related to the number of homes
E	estimated household electricity demand	L	grid extension distance
b_1	coefficient of the dispersed renewable energy source	H	number of homes
$d_{equalize}$	Equalize Distance	$P_{consumed}$	power consumption
LPL	Low priority lines	HLP	high priority lines
$P_{generation}$	power generation	P_{HPL}	power required by HPL
P_{LPL}	power required by LPL	CFL	energy saver
DC	direct current	AC	alternating current
COE	cost of energy	NPC	net present cost
C_A	annual cost	C_{Boilar}	boiler marginal cost
E_{Ther}	total thermal load	E_S	electric load served
CRF	capital recovery factor	i	real annual interest rate
f	annual inflation rate	LF	load-following
CC	cycle charging		

stations within the hybrid system. Additionally, it's important to highlight that the hybrid system incorporates storage systems, allowing the storage device to manage the load in cases of insufficient primary source capacity. Several storage alternatives are available, with rechargeable batteries and inertia flywheels being among the most commonly used. The hybrid system achieves greater efficiency through the integration of diverse renewable sources like solar and wind energy. Although renewable sources offer numerous benefits, it's essential to consider the ambient environmental factors, including factors such as solar radiation, temperature, and wind speed [9]. Due to these factors, many countries have sought to harness renewable resources, with China serving as a prominent example. China, in particular, has set out plans to expand its utilization of renewable resources [10]. Wind energy stands out as a pivotal renewable energy source adopted in numerous countries worldwide. Nonetheless, the intermittent and naturally fluctuating characteristics of wind power pose certain challenges [11]. It is crucial to incorporate wind power generation with other energy sources to enhance the stability of wind power generation and reduce the waste of wind energy [12]. These renewable energy methods have the potential to address current environmental challenges. Moreover, the key factor in designing HRES to meet the power quality, reliability, and energy needs of a specific area lies in the comprehension of its geographic, environmental, and regional climate characteristics [13].

Previously, a significant amount of research had been conducted to develop successful solutions focused on cost

optimization and the efficiency of Hybrid Renewable Energy Systems (HRES). The objective was to find optimal configurations that minimize costs while maximizing the utilization and performance of renewable energy sources within the system [14], Mixed-integer Quadratic programming technique[15], iterative technique[16], meta-PSO [17], genetic algorithm(GA) [18], Greedy Particle Swarm Optimization (GPSO) [19], probabilistic approach [20], and graphical construction technique [21]. Previous studies have reduced system efficiency while increasing costs. The study proposed in shows that for both sensitivity instances of 1.1 and $1.3/l of diesel, the analysis of the PV/diesel/battery hybrid renewable system configuration is found to be the best architecture[22]. For all climatic zones, the simulations focused on the net present costs, energy expenses, and renewable portion of the given hybrid setups.

The load demand of a typical microgrid system fluctuates on an hourly basis. In a microgrid system, HOMER software can be used to analyze and optimize the impact of time-of-consumption pricing on overall system performance. By incorporating pricing data and load profiles into the HOMER simulation, users can assess the potential benefits of load shifting and demand management strategies. Time-of-consumption-based electricity pricing takes into account these different load characteristics. By setting various rates at different times, utilities aim to incentivize consumers with an elastic load to shift their energy consumption away from peak demand periods. This approach helps balance the overall electricity demand and reduces strain on the grid during peak hours. Demand-Side Management (DSM) aims to shift elastic loads from peak load hours to hours when utility charges are lower. This strategy involves reshaping the entire demand model by leveraging the concept of demand-price elasticity. In [23] an advanced demand-shifting technique known as DSM was employed. The study utilized a day-ahead pricing strategy and an energy consumption game to investigate the application of the game theory-based DSM approach. The focus of the research was on a scenario involving a single utility and multiple residential energy consumers. By incorporating DSM into the MODEED problem, in [24] , the authors employed the Multi-objective Particle Swarm Optimization (MOPSO) technique to address the Multi-Objective Dynamic Economic and Emission Dispatch (MODEED) problem by integrating demand-side management (DSM). Moreover, the authors aimed to find optimal solutions that not only minimized economic costs but also reduced emissions by strategically managing the demand side of the power system. The MOPSO technique allowed for the simultaneous consideration of multiple objectives, such as economic cost and emissions, while finding the best compromise solutions. In[25] a contribution to advancing the field of home microgrid design and management by incorporating DSM has been presented. The collaborative optimization approach offers a comprehensive methodology for optimizing the operation and coordination of grid-connected home microgrids, ultimately leading to more efficient and sustainable energy systems.

The generating cost of a microgrid system is primarily influenced by two key factors: load demand and electricity market pricing. Therefore, when optimizing the operation of a microgrid system, it is crucial to consider not only the optimal scheduling of distributed generators but also the effective management of load demand, especially during periods of high power market prices. Demand Side Management (DSM) addresses this need by moving elastic loads during times of day when the electricity market price is lower. In a word, DSM decreases peak demand without reducing overall system load demand towards the end of the day. The suggested study provides an optimum, efficient, and cost-effective HRES setup considering DSM. Demand-side management (DSM) is frequent in smart grid networks due to its smart and quick capabilities of load shedding during peak demand hours. Researchers are attempting to optimize and conserve energy by implementing the DSM scheme on household equipment to control the load when the energy supply falls short of the energy demand for the residential load.

This study proposes an approach for designing a hybrid power system that takes into account an effective load control methodology. To assess the viability of the proposed hybrid power system, a remote area of Egypt (Qena-Hurghada) was selected. This research proposes a standalone hybrid power system for reducing the total cost of a microgrid system using the DSM technique. It is anticipated that a smart distribution board can switch between load lines automatically based on priority. The main contribution of this article is summarized as:

1. The suggested study provides an optimum, dependable, and cost-effective HRES implementation.

2. This study proposes an approach for designing a hybrid power system that takes into account an effective load control methodology.

3. A rural area of Egypt (Qena- Hurghada) was chosen to test the believability of the planned hybrid power system.

The rest of the paper is separated into the following categories: Proposed rural energy system design framework explained in Section 2. Study area and load assessment, in Section 3. Resources assessment discuss in Section 4 Mathematical modelling of HRES components is presented in Section 5, System Component in Section 6, Economic Parameters in Section 7, control strategy in Section 8, results and discussion in Section 9, optimum results in Section 10, system analysis in section 11 and Conclusions in Section 12.

2 Proposed rural energy system design framework

Fig. 1. illustrates the flowchart of the proposed algorithm [18]. Two priority load lines in the smart distribution board are Low Priority Load (LPL) and High Priority Load (HPL). The algorithm is set up so that LPL and HPL are always on during hours when power generation and consumption are equal. It feeds HPL and disconnects the LPL until total power generation surpasses the total power consumption of both lines, which happens when the total power generation is greater than the total power required by HPL but less than the total power consumption of both lines. Load shedding continues until LPL's power consumption exceeds its power generation, at which point all linked lines are disconnected. The system design load has been determined to be 284.16 kWh on HPL. The high-priority load consists of auxiliary appliances like electric iron, fan, energy saver, refrigerator, and motor pump based on the user's requirement and usage for daily purposes. Low-priority load lines consist of auxiliary appliances such as personal computers, low-wattage energy savers, TV, and washing machines as shown in Table 1.

3 Study area and load assessment

The Qena Governorate, located at latitude 26°10.2'N and longitude 32°46.7'E, offers favorable conditions for harnessing renewable energy resources. The region experiences ample sunshine throughout the year, making it conducive for solar power generation. Solar energy technologies, such as photovoltaic (PV) panels or Concentrated Solar Power (CSP) systems, can be deployed to capture the abundant solar radiation and convert it into electricity. Additionally, the area may have other renewable resources like wind or biomass that can be utilized for energy generation.

The Red Sea Governorate, situated at latitude 27°15.6'N and longitude 33°49'E, is another promising location for renewable energy development. The region is known for its coastal areas, which present opportunities for harnessing wind energy through offshore wind farms. The Red Sea's strong and consistent winds make it an ideal location for wind power generation. By installing wind turbines in strategic locations, the region can tap into this renewable resource and contribute to the overall energy mix.

Both Qena and the Red Sea Governorates offer significant potential for renewable energy deployment due to their geographical characteristics and the availability of solar

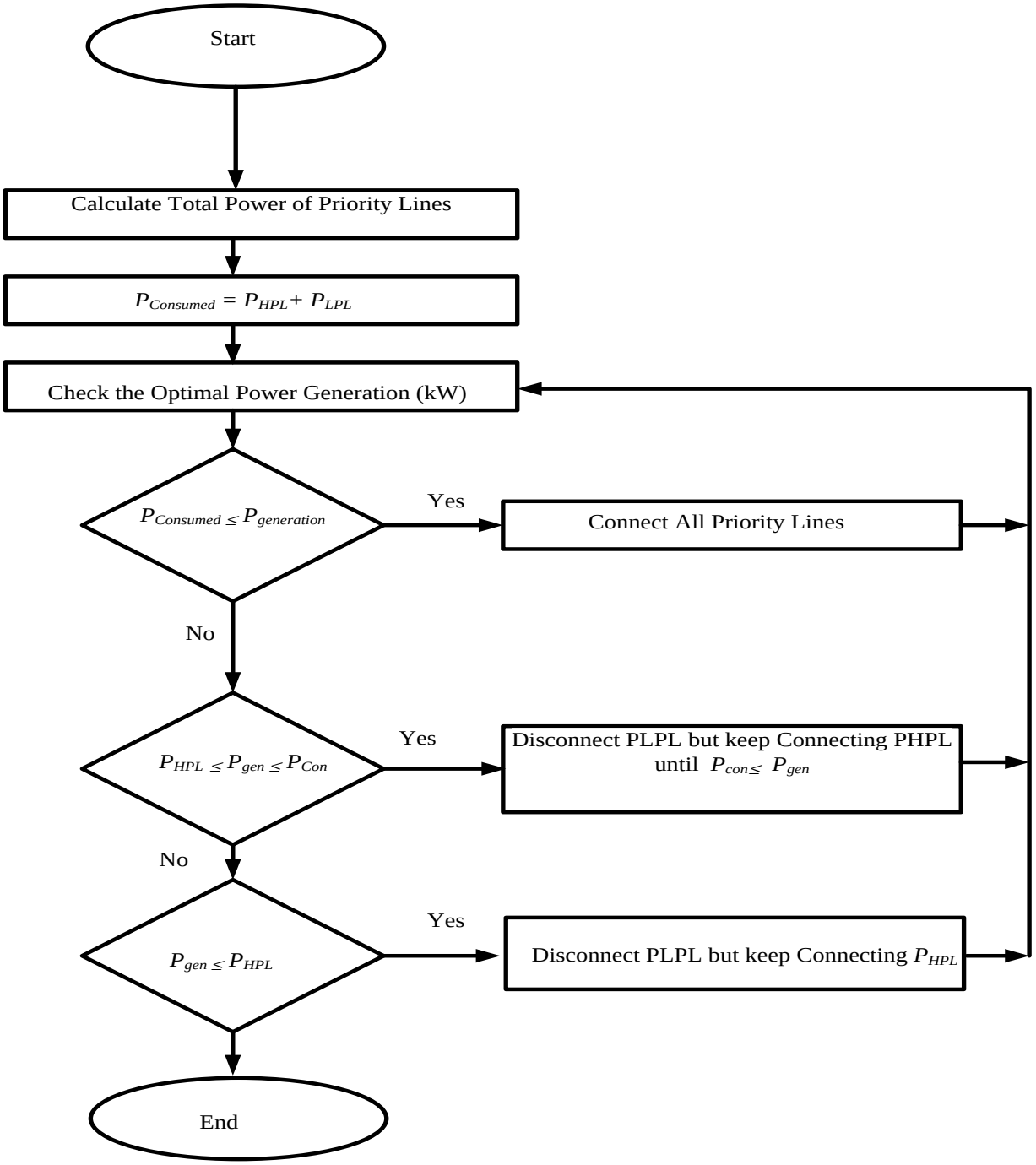

Fig.1 . Flowchart of the proposed algorithm.

and wind resources. Utilizing these renewable energy sources can lead to economic and reliable electricity generation in these regions, reducing reliance on traditional fossil fuel-based power generation and promoting a cleaner and more sustainable energy system. The amount of energy RETscreen Software[26] as shown in Table 2.

Table 1. Daily Residential load on priority lines

Appliances	HPL kWh/day	LPL kWh/day
Electric Iron	0.5	-
Fan	1.05	-
Personal Computer	-	0.4
Energy Saver (CFL) (40 w)	1.6	-
Energy Saver (CFL) (15 w)	-	0.3
Refrigerator	2.4	-
TV	-	0.75
Washing Machine	-	0.35
Motor Pump	0.37	-
Total	5.92	1.8

Table 2. Average Energy Demand for a Single Home (source: RETscreen Software).

Appliances	Load(W)	Quantity	Average Hourly usage/day	Energy demand		
				kWh/d	kWh/month	kWh/yr
Electric iron	1000	1	0.5	0.5	15	182.5
Fan	70	3	5	1.05	31.5	383.2
Personal Computer	200	1	2	0.4	12	146
Energy Saver(CFL)	40	4	10	1.6	48	584
Energy Saver(CFL)	15	2	10	0.3	9	109.5
Refrigerator	200	1	12	2.4	72	876
TV	150	1	5	0.75	22.5	273.7
Washing Machine	700	1	0.5	0.35	10.5	127.7
Motor Pump	370	1	1	0.37	11.1	135.05
Total	2745	18	46	7.72	231.6	2817.8

4 Resources assessment

To conduct the study, weather data from the Qena Governorate and Red Sea Governorate was obtained. The weather data included parameters such as Global Horizontal Irradiance (GHI), monthly average wind speed, and average monthly temperature. This data was extracted from NASA's weather data center module.

4.1 Qena Governorate climatic data assessment.

The first location considered in this study is the Qena Governorate, as depicted in Fig. 2. Fig. 2 illustrates the variations in the Global Horizontal Irradiance (GHI) and the clearness index. The annual average GHI is measured at 5.89 kWh/h/day, indicating the amount of solar radiation available for energy generation. The clearness index represents the transparency of the atmosphere in relation to solar radiation. Fig. 3 displays the average monthly temperature in Qena Governorate. The data reveals that the lowest average temperature occurs in January, measuring 13.49°C, while the highest average temperature is observed in July, reaching 32.72°C. These temperature variations throughout the year are crucial for understanding the climate conditions that impact energy generation and system performance.

In terms of wind energy potential, the region demonstrates promising characteristics. The average wind speed in Qena Governorate is recorded as 5.93 m/s, as depicted in Fig. 4. This suggests favorable conditions for harnessing wind

power. Furthermore, the data shows that June experiences the highest average wind speed at 6.82 m/s, indicating the peak wind resource availability during that month.

The detailed analysis of GHI, clearness index, average temperature, and wind speed in the Qena Governorate provides valuable insights into the renewable energy potential of the region. These parameters serve as essential inputs for evaluating the feasibility and performance of solar and wind energy systems. By considering these factors, researchers and decision-makers can make informed decisions regarding the design and implementation of renewable energy projects in Qena Governorate.

4.2 Red Sea Governorate climatic data assessment.

The second location considered in this study is the Red Sea Governorate. Fig. 5 depicts the variations in the Global Horizontal Irradiance (GHI) and the clearness index for the studied location. The annual average GHI is measured at 5.93 kWh/h/day, representing the amount of solar radiation available for energy generation. The clearness index provides insights into atmospheric transparency in relation to solar radiation. Fig. 6 shows the average monthly temperatures for the location under consideration. According to the data, the lowest average temperature occurs in January, measuring 16.69°C. On the other hand, the highest average temperature is observed in August, reaching 30.6°C. These temperature variations throughout the year play a significant role in assessing the climatic conditions that impact energy generation and system performance.

The detailed analysis of GHI, clearness index, and average temperatures depicted in Fig. 5 and 6 provide valuable information about the renewable energy potential of the studied location. These parameters are crucial for evaluating the feasibility and performance of solar energy systems. By considering these factors, researchers and decision-makers can make informed decisions regarding the design and implementation of solar energy projects in the given area. In the studied region, the average wind speed is recorded as 7.13 m/s, as shown in Fig. 7. This indicates the general wind resource potential available for energy generation. Additionally, the data reveals that August experiences the highest average wind speed at 8.32 m/s. These variations in wind speed throughout the year are essential in assessing the suitability and potential for harnessing wind energy in the region.

5 Mathematical modelling of HRES components

The Hybrid Renewable Energy System (HRES) described in the study has been modeled using the following mathematical equations.

5.1 PV system modelling

According to Harvard, the following mathematical equations can be used to determine the output power of a solar photovoltaic (PV) generator [27]:

$$P_{PV} = N \times A_m \times \eta_g \times G_t \quad (1)$$

where P_{PV} represents the output power of the solar PV generator, N is the total number of solar PV modules. A_m represents the total area of the PV modules, measured in m^2. G_t represents the solar irradiance or solar radiation incident on the PV modules, measured in watts per m^2. η_g the PV generator's efficiency.

These mathematical equations provide a framework for estimating the output power of a solar PV generator based on inputs such as the system efficiency, module area, solar irradiance, and solar radiation. By utilizing these equations, researchers and engineers can assess the expected power output of a solar PV system under different environmental conditions and system configurations. This information is crucial for system design, performance analysis, and energy yield estimation, contributing to the effective utilization of solar energy resources.

ηg determines the efficiency of PV generators using the following equation [28]:

$$\eta_g = \eta_{Pt}\eta_r \left[1 - (T_C - T_r)\beta_t - G_t\beta_t\left(\frac{NOCT - 20}{800}\right)(\eta_{Pt}\eta_r)\right] \quad (2)$$

where, η_g the PV generator's efficiency, η_{Pt} the power point tracker's efficiency, η_r the generator's reference efficiency, T_C the PV cell's temperature, T_r is the reference temperature of the PV cell, β_t is the temperature coefficient of efficiency and NOCT is the nominal operating cell temperature.

5.2 Wind turbine modelling

Eq.(3) shows the estimated mathematical model of a wind turbine:

$$P_{WT} = \begin{cases} 0 & v_{out} < v < v_{in} \\ \left(\frac{v - v_{in}}{v_n - v_{in}}\right) P_m & v_{in} < v < v_n \\ P_m & v_n < v < v_{out} \end{cases} \quad (3)$$

where, v is the wind speed, v_{in} is the wind's cut-in speed, The wind's rated speed is v_n, its cutoff speed is v_{out}, and the wind turbine's rated power is P_m. When the wind speed is either lower than cut in speed or higher than cut out speed, wind turbine power (P_{wt}) is zero. If the wind speed is less than the rated speed, the power of the wind turbine is directly proportional to the wind speed [29].

Grid extension's Levelized Cost of Electricity (LCOE) is defined in (4) and the levelized cost of electricity for HRES is defined in (5) [18]:

$$LCOE_{grid} = LRMC + \frac{a_1 L + a_2 H}{E} \quad (4)$$

$$LCOE_{HRES} = \frac{b_1 H}{E} \quad (5)$$

where LRMC stands for the long-run marginal cost of electricity in \$/kWh, a_1 represents the grid extension constant related to distance in \$, a_2 represents the grid extension constant related to the number of homes in \$, E represents the estimated household electricity demand in kWh, L represents the grid extension distance in km, b_1 represents the coefficient of the dispersed renewable energy source in \$, and H represents the number of homes in the remote area.

The following is the rational way to equalize the distance between grid extensions and hybrid renewable energy systems $(d_{equalized})$ [18]:

$$d_{equalize} = \frac{(b_1 - a_1 LRMC \times E)H}{a_1} \quad (6)$$

6 System Component

6.1 PV panel

The data regarding the PV panel used in the study was obtained from ref. [8]. The cost associated with the PV panel is as follows: \$1420.7 per kW for the initial investment, \$1420.7 per kW for replacement, and \$30.2 per year for operation and maintenance. To account for the derating factor, the total PV production is reduced by 20%. The derating factor represents various factors that affect the performance of the PV panel, such as temperature and dust. In this study, the derating factor is set to 80% of the total PV production. By applying the derating factor, the study considers a 20% reduction in PV production. This adjustment accounts for the impact of temperature, dust, and other factors on the actual performance of the PV panel. It helps in providing more accurate estimations and predictions of the PV system's energy output and overall performance. Considering these cost and derating factor parameters, the study can evaluate the economic feasibility, operation, and maintenance costs associated with the PV panel. Additionally, the adjustment made through the derating factor allows for a more realistic assessment of the PV panel's performance under various conditions and helps in optimizing system design and operation.

6.2 Wind turbine

The data related to the wind turbine used in this study is sourced from ref. [8]. The following details are associated with this particular type of wind turbine:

- Investment cost: \$1097 per kilowatt (kW)
- Replacement cost: \$1097 per kW
- Operation and maintenance cost: \$10.97 per year

These costs represent the financial aspects associated with the wind turbine, including the initial investment, future replacement, and ongoing operation and maintenance expenses. Several significant considerations make this wind turbine attractive for the study. These include its affordability, low start-up wind speed, and extended warranty periods. The low price of the wind turbine makes it an economically viable option, while the low start-up wind speed allows it to begin generating power even at relatively low wind velocities. The lengthy warranty periods provide additional assurance regarding the performance and durability of the wind turbine. The wind turbine power curve is shown in Fig. 8.

6.3 Diesel Fuel

In certain remote areas, diesel generators serve as the primary source of electricity. In such cases, minimal civil effort is required. To produce 1 kW of power using a diesel generator, a capital cost of \$600 is necessary. Additionally, a replacement cost estimate of \$500 per kW is used. These cost figures represent the financial considerations associated with the deployment and operation of diesel generators in remote areas. The initial capital cost of \$600 is the investment required to acquire a diesel generator capable of producing 1 kW of power. This cost includes the purchase and installation expenses. Furthermore, a replacement cost estimate of \$500 per kW is considered for future replacements or upgrades of the diesel generator.

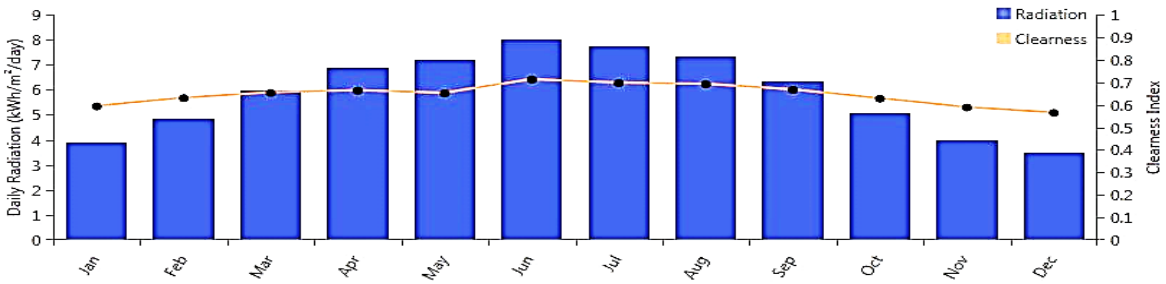

Fig. 2. Average monthly solar radiation kW h/m2/day and clearness index

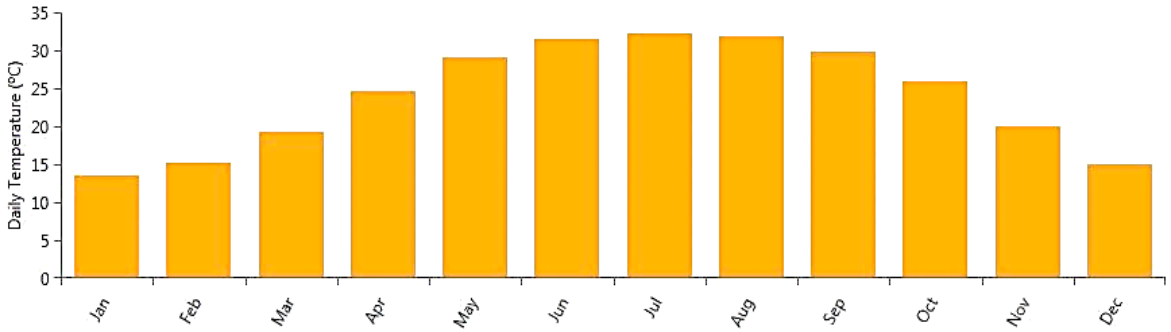

Fig. 3. The monthly average temperature of Qena Governorate

Fig. 4. Average monthly solar wind speed (m/s).\

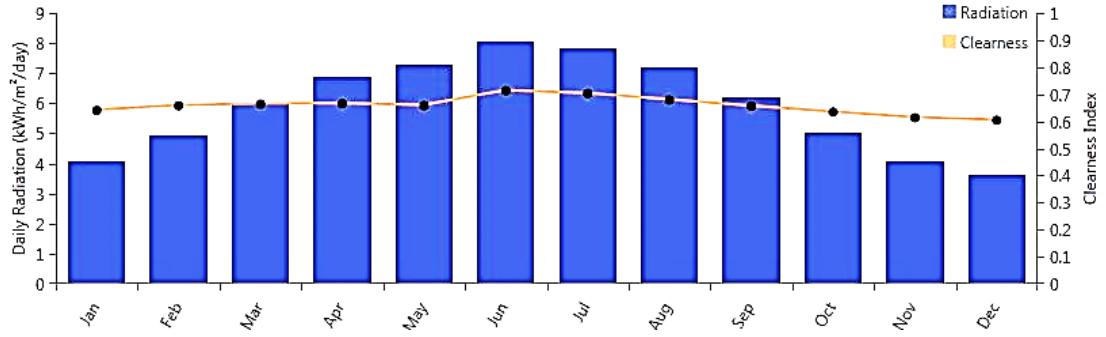

Fig. 5. Average monthly solar radiation kW h/m2/day and clearness index

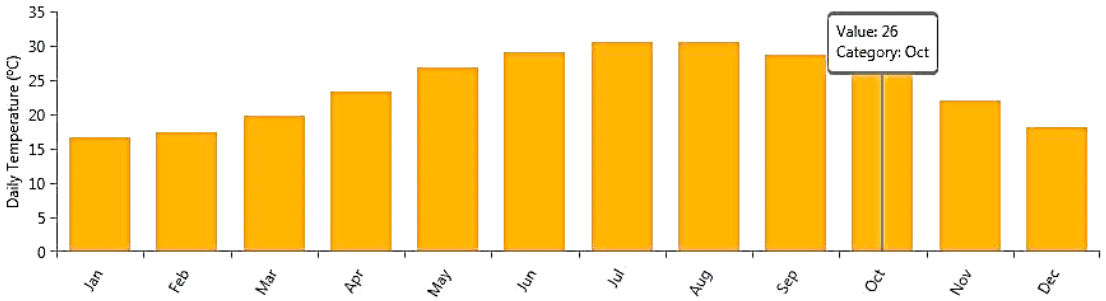

Fig. 6. The monthly average temperature of Qena Governorate

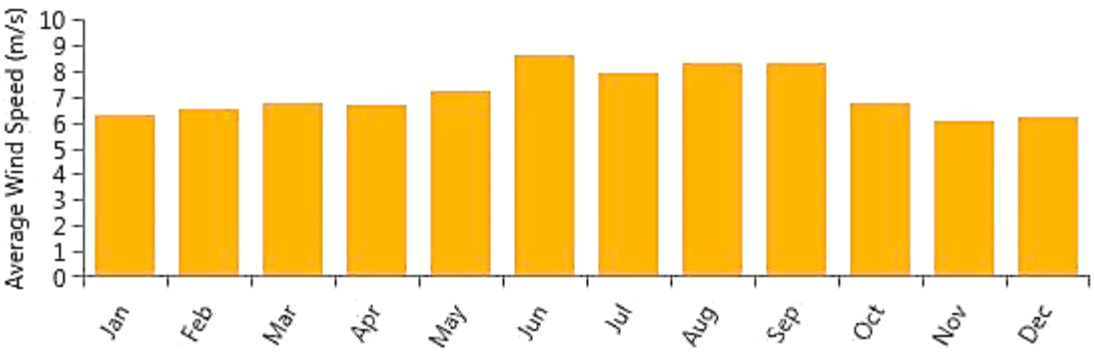

Fig. 7 Average monthly wind speed (m/s)

This accounts for the cost of replacing the existing generator with a new one or increasing its capacity. By taking these cost factors into account, the study evaluates the economic feasibility and operational expenses associated with the diesel generator as an electricity source in remote areas. This information aids in understanding the financial implications and helps in decision-making regarding the deployment and maintenance of diesel generator systems. The generator's operating and maintenance costs are calculated at $0.025/hour/kW.

Considering the price on the market right now, $0.77 per liter of diesel [30].

6.4 Battery

During the daytime, energy storage is achieved through the use of batteries. In this hybrid system, a generic 1 kilowatt-hour (kWh) lead acid battery (1 kWh LA) is employed as the storage component. The lead acid battery serves as a means to store excess energy generated by renewable sources during daylight hours. It allows for the accumulation of energy when the generation exceeds the demand, which can then be utilized during periods when the demand surpasses the renewable generation capacity. Each battery in the system has a maximum capacity of 83.4 ampere-hours (Ah) and a nominal capacity of 1 kilowatt-hour (kWh) with a nominal voltage of 12 volts (V). The maximum charge current is 16.7 amperes (A), while the maximum discharge current is 24.3 A. In terms of longevity, each battery has a lifespan of ten years. The investment cost and replacement price for each battery are both $300. These costs represent the initial investment required to acquire and install each battery, as well as the cost of replacing a battery at the end of its lifespan. Additionally, an estimated annual operating and maintenance expense of $10 is associated with each battery. This expense covers routine maintenance, monitoring, and other operational costs incurred over the course of a year [30].

6.5 Converter

In this study, an inverter is utilized to convert the direct current (DC) output of the PV panels into usable alternating current (AC) electricity. The design of the inverter used in the study incorporates the following specifications:

- **Cost:** The inverter is designed to cost $600. This cost reflects the initial investment required to acquire and install the inverter.

- **Warranty:** The inverter comes with a 15-year warranty. This warranty period ensures that any faults or malfunctions within the specified timeframe are covered and can be repaired or replaced without additional cost.

- **Replacement cost:** In the event that the inverter needs to be replaced, the cost is estimated to be $600. This replacement cost accounts for acquiring and installing a new inverter if the existing one becomes defective or reaches the end of its lifespan.

- **Operation and maintenance cost:** The inverter has an estimated annual operation and maintenance cost of $30. This cost covers the routine upkeep, monitoring, and servicing of the inverter throughout the year.

- **Efficiency:** The inverter and rectifier are assumed to have efficiencies of 90% and 85%, respectively. These efficiency values indicate the conversion efficiency of the inverter in converting DC power to AC power and the efficiency of the rectifier in converting AC power to DC power.

By incorporating these design specifications, the study evaluates the economic implications, performance, and maintenance requirements of the inverter in the overall system. The efficiency values provide an understanding of the energy losses that occur during the conversion process and assist in assessing the overall system efficiency [31].

7 Economic Parameters

In this study, the project's lifetime is set at 25 years. Throughout the analysis, the optimum combination of Hybrid Renewable Energy Systems (HRES) is determined based on two key metrics: the lowest Cost of Energy (COE) and the lowest Net Present Cost (NPC). The COE represents the cost per unit of electrical energy consumed by the HRES over the course of a year. It takes into account the total costs associated with the various components of the system, including renewable energy sources, storage, inverters, and any additional equipment. By minimizing the COE, the aim is to achieve the most cost-effective operation of the HRES. Additionally, the NPC is considered in determining the optimal HRES combination. The NPC takes into account the present value of all costs and benefits associated with the project over its entire lifetime, discounted to its current value. By minimizing the NPC, the study aims to identify the combination of HRES components that provides the most economically viable solution. During the analysis, the cost associated with the thermal energy generation from the boiler is subtracted from the yearly cost. This accounts for the cost savings achieved by utilizing thermal energy generated by the boiler, resulting in a reduction in the overall yearly cost. By considering both the COE and

NPC as evaluation criteria, the study identifies the optimal HRES combination that offers the lowest overall cost and highest economic viability over the 25-year project lifetime. This information assists in decision-making regarding the design and implementation of the HRES to ensure the most efficient and cost-effective utilization of renewable energy resources. The HOMER software determines the COE in an HRES where thermal energy is provided by a fuel-fired boiler using Eq. (7) [18, 32-39]:

$$COE = \frac{C_A - C_{Boilar} E_{Ther}}{E_s} \quad (7)$$

where C_A is the annual cost (\$/yr.), C_{Boilar} is the boiler marginal cost (\$/kWh), E_{Ther} is the total thermal load served (kWh/yr), and E_S is the electric load served (kWh/yr). The NPC is calculated using Equation (8). as CRF (i, n) is the capital recovery factor which is calculated from Eq.(9):

$$NPC = \frac{C_A}{CRF(i\,, n)} \quad (8)$$

$$\mathrm{CRF}(i\,, n) = \frac{i(1+i)^n}{(1+i)^n - 1} \quad (9)$$

The real interest rate is the nominal difference between the interest rate and the inflation rate. The real annual interest rate i is determined by Eq.(10) [40].

where i' is the nominal interest rate, and f is the annual inflation rate.

$$i = \frac{i - f}{1 + f} \quad (10)$$

8 Control strategy

In this study, the HOMER Pro software is utilized with two separate control schemes: load following and cycle charging. These control schemes determine how the generator operates to meet the electricity demand of the system. Under the load-following (LF) strategy, the generator only produces the necessary amount of power to meet the current demand. This approach is suitable for systems with a significant amount of renewable with a significant amount of renewable electricity that occasionally exceeds the load. By closely following the load, the system can effectively utilize the available renewable energy without wasting excess generation. In the tables of the results, the load following strategy is represented by the symbol "LF". On the other hand, the cycle charging strategy involves running the generator at maximum power when it is called upon, and any excess capacity is used to charge the battery bank. This strategy is more suitable for systems with limited or no renewable energy sources. By maximizing generator output and utilizing excess capacity for battery charging, this strategy ensures efficient utilization of the generator's potential. In the tables of the results, the cycle charging strategy is indicated by the symbol "CC". For this investigation, the load-following approach is employed. It implies that the generator will adjust its output based on the load demand, ensuring that it meets the required electricity demand while minimizing wastage. This choice is made based on the specific characteristics of the system and the availability of renewable energy sources. By employing the load-following strategy in the analysis, the study assesses the performance and cost-effectiveness of the hybrid system under this control scheme. The results obtained help in understanding the system's operation and optimizing its efficiency for the given set of conditions.

9 Results and discussions

To identify the optimal combination of renewable resources in the lowest cost of energy supply, the two scenarios are considered. In the first scenario, the full load is applied (without applied DSM) and then a demand-side management (DSM) strategy is implemented in the second scenario. These scenarios are evaluated for both the Qena and Red Sea governorates. The section is divided into three distinct scenarios, and each scenario is applied to both governorates. The aim is to compare the costs of energy supply and select the system with the lower cost. By conducting this analysis, the study seeks to determine the most cost-effective combination of renewable resources for each scenario and location. The analysis takes into account various factors such as the availability and suitability of renewable energy sources, the associated capital and operational costs, and the overall system performance. By considering these factors, the study aims to identify the optimal renewable resource combination that minimizes the cost of energy supply while meeting the desired load requirements.

The results obtained from this analysis provide valuable insights into the economic feasibility and the effectiveness of different renewable resource combinations in the specific contexts of Qena and Red Sea governorates. This information can guide decision-making processes and assist in designing and implementing sustainable and cost-efficient energy systems in these regions. Therefore, this part was divided into three scenarios, and each scenario

is applied in the two governorates, and the system with a lower cost is selected.

- Scenario 1: Diesel only
- Scenario 2: HRES without DSM
- Scenario 3: HRES with DSM

9.1 Scenario # 1: Diesel only

In this scenario, a diesel generator only is used to feed the loads, where the electricity demand is met by diesel generators. The total designed electrical load is 370.56 kWh per day, and it is assumed that this load will be supplied by the diesel generator. This type of setup is commonly used in remote or off-grid locations where the grid connection is not feasible or reliable. Diesel generators serve as the primary source of power in this system. The HOMER software can be employed to analyze and optimize the performance and economics of the system. By inputting the load demand, diesel generator specifications, fuel costs, and other relevant parameters, HOMER can provide valuable insights into the system's operation and help in identifying the most efficient and cost-effective configuration. By utilizing HOMER, one can explore various aspects of the diesel-fed load system, such as generator sizing, fuel consumption, system reliability, and overall economics. The software can perform simulations, conduct sensitivity analyses, and optimize the system design to find the best configuration that meets the load demand while minimizing costs and ensuring a reliable power supply. By utilizing the capabilities of HOMER, decision-makers and system designers can make informed choices regarding the sizing, operation, and management of the diesel-fed load system. This allows for the optimization of performance, cost-effectiveness, and reliability, ensuring that the system meets the electricity demand efficiently in locations where grid connection is not feasible or reliable. Fig. 9 shows a schematic diagram of HOMER for scenario #1.

9.2 Scenario #2: HRES without DSM

As mentioned in the previous scenario, the overall designed electrical load is 370.56 kWh per day. To fulfill this load demand, a combination of different sources is employed, including photovoltaic (PV) cells, wind turbines, batteries, and diesel generators. The schematic diagram of the system configuration is depicted in Fig. 10. Fig. 10 shows the different components interconnect to meet electricity demand. The PV cells convert solar energy into electricity, while wind turbines harness the power of the wind to generate electricity. These renewable energy sources provide clean and sustainable power to the system. Additionally, batteries are incorporated into the system to store excess energy generated by PV cells and wind turbines. These batteries play a crucial role in balancing the supply and demand of electricity by storing energy during periods of high generation and supplying it during times of low generation or high demand. Furthermore, to ensure continuous power supply and to meet the load demand when renewable sources are insufficient, diesel generators are integrated into the system. These generators provide backup power and can be activated when the renewable sources are unable to meet the required electricity demand. By combining these different sources and utilizing storage capabilities, the system aims to optimize the use of renewable energy while ensuring a reliable and continuous power supply. The schematic diagram provides an overview of how the components are integrated and work together to meet the overall designed electrical load of 370.56 kWh per day.

9.3 Scenario #3: HRES with DSM

In this scenario, the total designed electrical load of 370.56 kWh per day has been reduced by the load of the High Power Load (HPL), which amounts to 284.16 kWh per day. In Fig. 11, a hybrid system is employed to meet the remaining load demand. The hybrid system comprises various renewable resources, including photovoltaic (PV) cells and wind turbines, as well as energy storage in batteries, and backup power from diesel generators. These components are integrated to ensure a reliable and continuous power supply. In situations where renewable sources are unable to meet the load demand or during periods of high demand, diesel generators are activated to provide backup power. This ensures that the electricity demand is consistently met, even under challenging conditions. The hybrid system's configuration depicted in Fig. 11 demonstrates the integration of these renewable resources, energy storage, and backup power sources. By utilizing a combination of these components, the system aims to optimize the use of renewable energy, enhance system reliability, and meet the reduced electrical load demand effectively.

10 Optimum Results

10.1 Optimal system for diesel generator

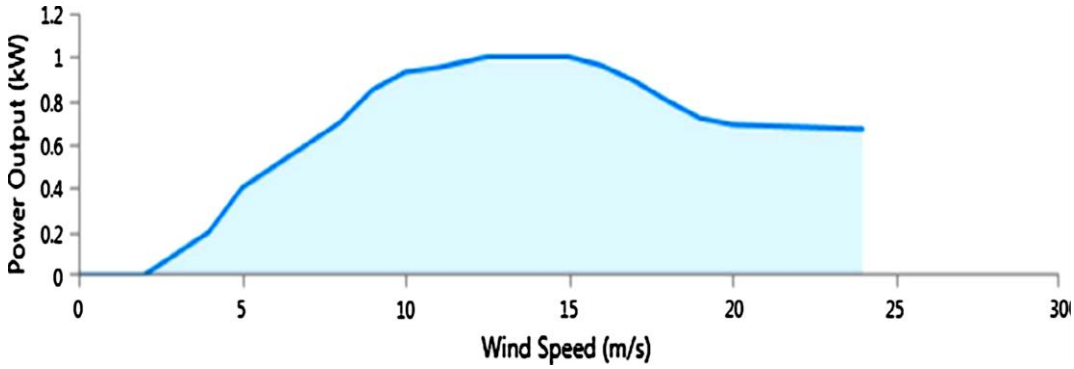

Fig. 8. Wind turbine power curve

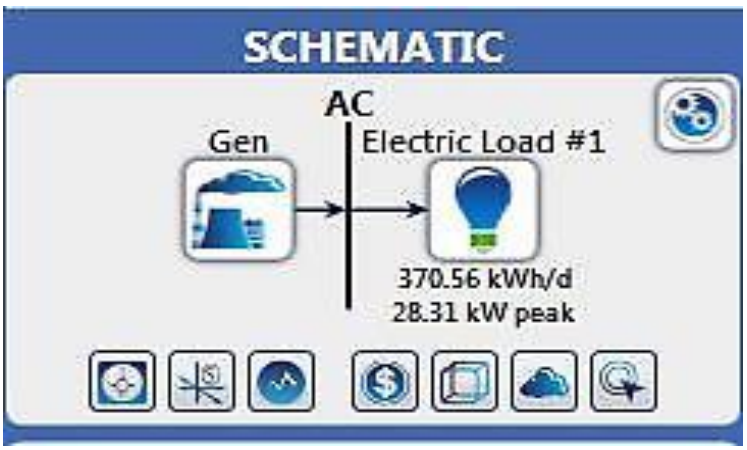

Fig.9. Schematic Diagram of HOMER for Diesel Generator

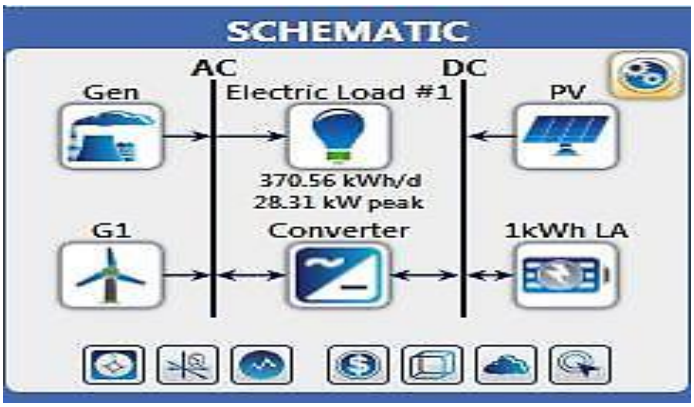

Fig.10. Schematic Diagram of HOMER for HRES without DSM

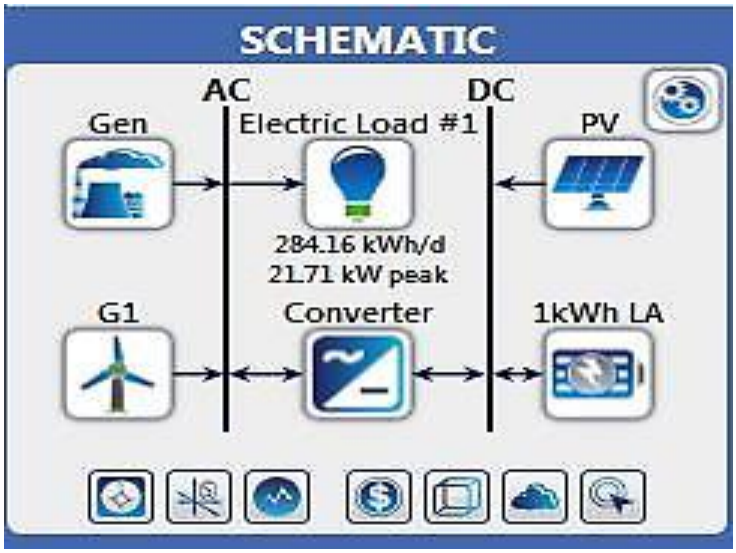

Fig.11. Schematic Diagram of HOMER for HRES with DSM

The optimal solution for scenario #1 is presented in Fig.12. The Cost of Energy (COE) is determined to be 0.391 dollars per kilowatt-hour (kWh), and the Net Present Cost (NPC) is calculated as 1.60 million dollars. In this system configuration, the unmet electric load is 0%, indicating that the system successfully meets the entire load demand. Fig. 13 illustrates the electrical production summary for the diesel generator obtained from the HOMER Pro software. The data indicates the performance and output of the diesel generator within the system. The results demonstrate that the system's design and component integration enables the diesel generator to effectively meet the load demand, resulting in no unmet electric load. Considering these outcomes, this system configuration proves to be the optimal choice for implementation in both Qena and Red Sea Governorates. With a relatively low cost of energy and no unmet load, it offers a cost-effective and reliable solution for meeting the electricity demand in these regions.

10.2 Optimal system for HRES without DSM

In this scenario, the optimal solution is depicted in Fig. 14. The COE value is calculated as 0.214 dollars per kilowatt-hour (kWh) for the total system in the Qena Governorate. Additionally, the NPC value for this system is determined as 874,443 dollars. Similarly, for the system applied in the Red Sea Governorate, the COE value is 0.183 dollars per kWh, while the NPC value is 747,329 dollars, as shown in Fig. 15. These results demonstrate that the proposed hybrid systems offer cost-effective energy solutions when compared to the diesel system alone. Furthermore, the unmet electric load for both locations is 0%, indicating that the hybrid systems effectively meet the entire load demand. This is confirmed by examining the electrical production summary for the diesel generator obtained from the HOMER Pro software, as illustrated in Fig. 16 for the Qena Governorate and Fig. 17 for the Red Sea Governorate.

The achieved COE and NPC values for both governorates signify the economic feasibility of the proposed systems. With no unmet electric load, these systems provide a reliable electricity supply while ensuring cost efficiency. These results underscore the superiority of the hybrid system configuration over the diesel-only system in terms of both cost and performance in the Qena and Red Sea Governorates.

10.3 Optimal system for HRES with DSM

In the case of considering demand-side management (DSM) in the hybrid renewable energy systems (HRES), the cost of energy (COE) value is determined as $0.212, and the net present cost (NPC) value is $665,267 for the Qena Governorate, as shown in Fig. 18. Similarly, for the Red Sea Governorate, the COE value is $0.181, and the NPC value is $569,353, as illustrated in Fig. 19. It is worth noting that when DSM is applied, the COE and NPC values are lower compared to the HRES without DSM and the diesel generator system. Furthermore, the unmet electric load for both locations is 0%, indicating that the hybrid systems with DSM effectively meet the entire load demand.

This is evident from the electrical production summary depicted in Fig. 20 for the Qena Governorate and Fig. 21 for the Red Sea Governorate.

The achieved COE and NPC values in the presence of DSM highlight the cost-effectiveness and economic feasibility of integrating demand-side management techniques into hybrid renewable energy systems. The results demonstrate the advantages of incorporating DSM in terms of reducing energy costs and optimizing the overall performance of the systems, leading to a more reliable and sustainable electricity supply.

11 System analysis

The power system configurations in this study were determined through sensitivity analysis and optimization methods using HOMER Pro software. Energy balancing calculations were conducted for each power system design based on the data provided by HOMER Pro. The net present cost was used as a metric to compare the cost of different system designs, and HOMER Pro software facilitated the sorting and analysis of the results [41]. The simulation output compared four main case studies: the diesel generator system, the HRES without DSM, and the HRES with DSM. These systems were applied in remote areas within two governorates in the Arab Republic of Egypt. Tables 4 and 5 present a comparison of the three systems in the two governorates, clearly demonstrating that the HRES with DSM is the best option among the suggested hybrid system configurations. Table 8 provides additional details on the comparison study. The comparison study highlights that the hybrid renewable energy system (HRES) with Demand-Side Management (DSM) is the most favorable choice for remote areas. Implementing DSM not only contributes to reducing economic costs but also enhances the overall performance and efficiency of the power systems. This finding emphasizes the significance of integrating renewable energy sources with DSM techniques to achieve sustainable and cost-effective solutions for remote areas.

12 Conclusion

Demand-side management control is implemented to minimize unnecessary investments in the power plant and optimize the load profile for off-grid systems. When comparing the proposed system design with the conventional hybrid system, the diesel generators show consistent and highest generation costs ($0.391/kWh) and a net present cost of $1.6 million when applied in the two governorates. The proposed demand-side management system proves to be more favorable, particularly in Qena governorate, where it reduces the initial capital cost of the system by 24.1%. The cost of energy (COE) decreases by 0.93% from $0.214/kWh to $0.212/kWh, and the net present cost (NPC) improves from $874,443 to $665,267, reflecting a reduction of 23.9%. Similarly, in the case of the Red Sea governorate, the cost of energy (COE) decreases by 1.1% from $0.183/kWh to $0.181/kWh, and the net present cost (NPC) improves from $747,329 to $569,353, indicating a reduction of 23.8%. Considering the availability and accessibility of renewable resources in the Arab Republic of Egypt at low cost/kWh, it is highly recommended to adopt the proposed hybrid renewable energy management system (HRES) with demand-side management (DSM) to meet the growing energy demand. This approach is more favorable than relying solely on the national grid or expanding the capacity of diesel power plants with high generation costs/kWh. Future research endeavors will focus on addressing the supply-load imbalance by exploring different types of power electronics circuits and implementing a more advanced energy management system. These efforts aim to enhance the system's response time and overall efficiency, further improving the performance of the hybrid renewable energy management system with demand-side management.

Export...

Optimization Results

Left Double Click on a particular system to see its detailed Simulation Results.

Architecture			Cost				System		Gen				
	Gen (kW)	Dispatch	NPC ($)	COE ($)	Operating cost ($/yr)	Initial capital ($)	Ren Frac (%)	Total Fuel (L/yr)	Hours	Production (kWh)	Fuel (L)	O&M Cost ($/yr)	Fuel Cost ($/yr)
	32.0	LF	$1.60M	$0.391	$52,310	$19,200	0	47,621	8,760	135,407	47,621	7,008	36,668

Fig.12. Optimization Results for Diesel

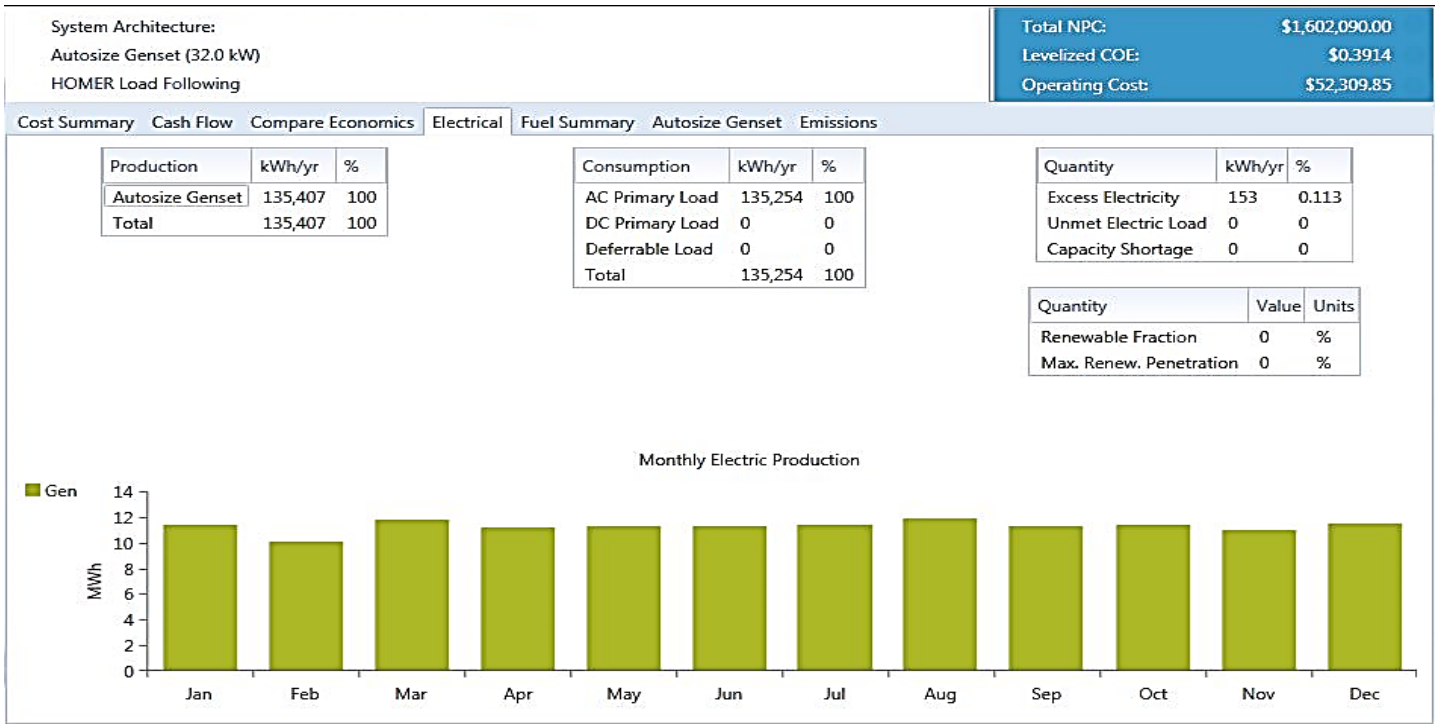

Fig.13. Electrical Production Summary for Diesel

Export...

Optimization Results

Left Double Click on a particular system to see its detailed Simulation Results.

Architecture											Cost				System	
					PV (kW)	G1	Gen (kW)	1kWh LA	Converter (kW)	Dispatch	NPC ($)	COE ($)	Operating cost ($/yr)	Initial capital ($)	Ren Frac (%)	Total Fuel (L/yr)
					36.3	91	32.0	115	23.4	LF	$874,443	$0.214	$21,889	$212,079	74.2	12,471
						135	32.0	114	15.2	LF	$973,979	$0.238	$25,377	$206,060	66.6	16,244
						155	32.0			CC	$1.16M	$0.283	$32,029	$189,235	52.5	25,018
					0.766	155	32.0		0.486	CC	$1.16M	$0.283	$32,008	$190,469	52.8	24,938
					116	99		618	29.4	CC	$1.18M	$0.289	$23,631	$466,993	100	0
					72.9		32.0	149	26.5	LF	$1.20M	$0.293	$33,804	$175,398	48.2	24,401
					18.4		32.0		10.6	CC	$1.54M	$0.377	$49,388	$48,510	15.6	42,590
							32.0			CC	$1.60M	$0.391	$52,310	$19,200	0	47,621
							32.0	3	0.224	CC	$1.61M	$0.392	$52,401	$20,167	0	47,621
					232			1,091	106	CC	$1.95M	$0.477	$41,759	$688,042	100	0
						569		1,821	29.9	CC	$3.08M	$0.753	$62,858	$1.18M	100	0

Fig. 14. Optimization Results for HRES without DSM in Qena governorate

Export...

Optimization Results

Left Double Click on a particular system to see its detailed Simulation Results.

Architecture											Cost				
						PV (kW)	G1	Gen (kW)	1kWh LA	Converter (kW)	Dispatch	NPC ($)	COE ($)	Operating cost ($/yr)	Initial capital ($)	Ren Frac (%)
						28.0	90	32.0	120	21.0	LF	$747,329	$0.183	$17,881	$206,256	80.6
							124	32.0	82	13.9	LF	$790,739	$0.193	$19,913	$188,169	74.2
⚠							131	32.0			CC	$963,527	$0.235	$26,458	$162,907	61.4
⚠						0.156	123	32.0		0.170	CC	$965,551	$0.236	$26,804	$154,455	60.6
						78.3	165		494	27.9	CC	$1.08M	$0.264	$20,589	$457,223	100
						68.7		32.0	150	26.0	LF	$1.20M	$0.293	$33,832	$177,423	48.3

Fig.15. Optimization Results for HRES without DSM in Red Sea governorate

System Architecture: Autosize Genset (32.0 kW) HOMER Load Following
Generic flat plate PV (36.3 kW) Generic 1kWh Lead Acid (115 strings)
Generic 1 kW (91.0) System Converter (23.4 kW)

Total NPC:	$874,442.90
Levelized COE:	$0.2137
Operating Cost:	$21,889.17

Generic 1 kW | System Converter | Emissions

Cost Summary | Cash Flow | Compare Economics | Electrical | Fuel Summary | Autosize Genset | Renewable Penetration | Generic 1kWh Lead Acid | Generic flat plate PV

Production	kWh/yr	%
Generic flat plate PV	66,358	21.8
Autosize Genset	34,930	11.5
Generic 1 kW	202,611	66.7
Total	303,899	100

Consumption	kWh/yr	%
AC Primary Load	135,254	100
DC Primary Load	0	0
Deferrable Load	0	0
Total	135,254	100

Quantity	kWh/yr	%
Excess Electricity	161,876	53.3
Unmet Electric Load	0	0
Capacity Shortage	0	0

Quantity	Value	Units
Renewable Fraction	74.2	%
Max. Renew. Penetration	2,161	%

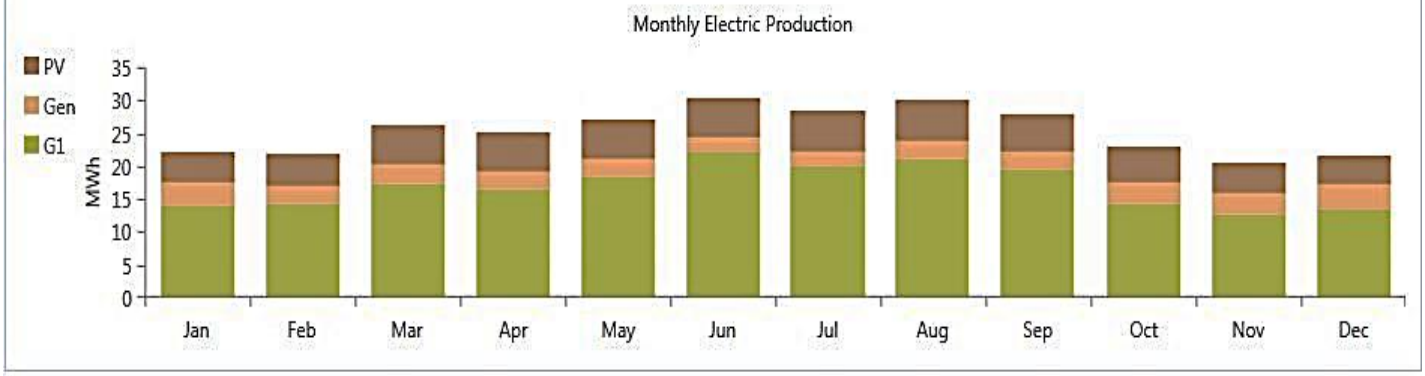

Fig. 16. Electrical Production Summary for HRES without DSM in Qena governorate

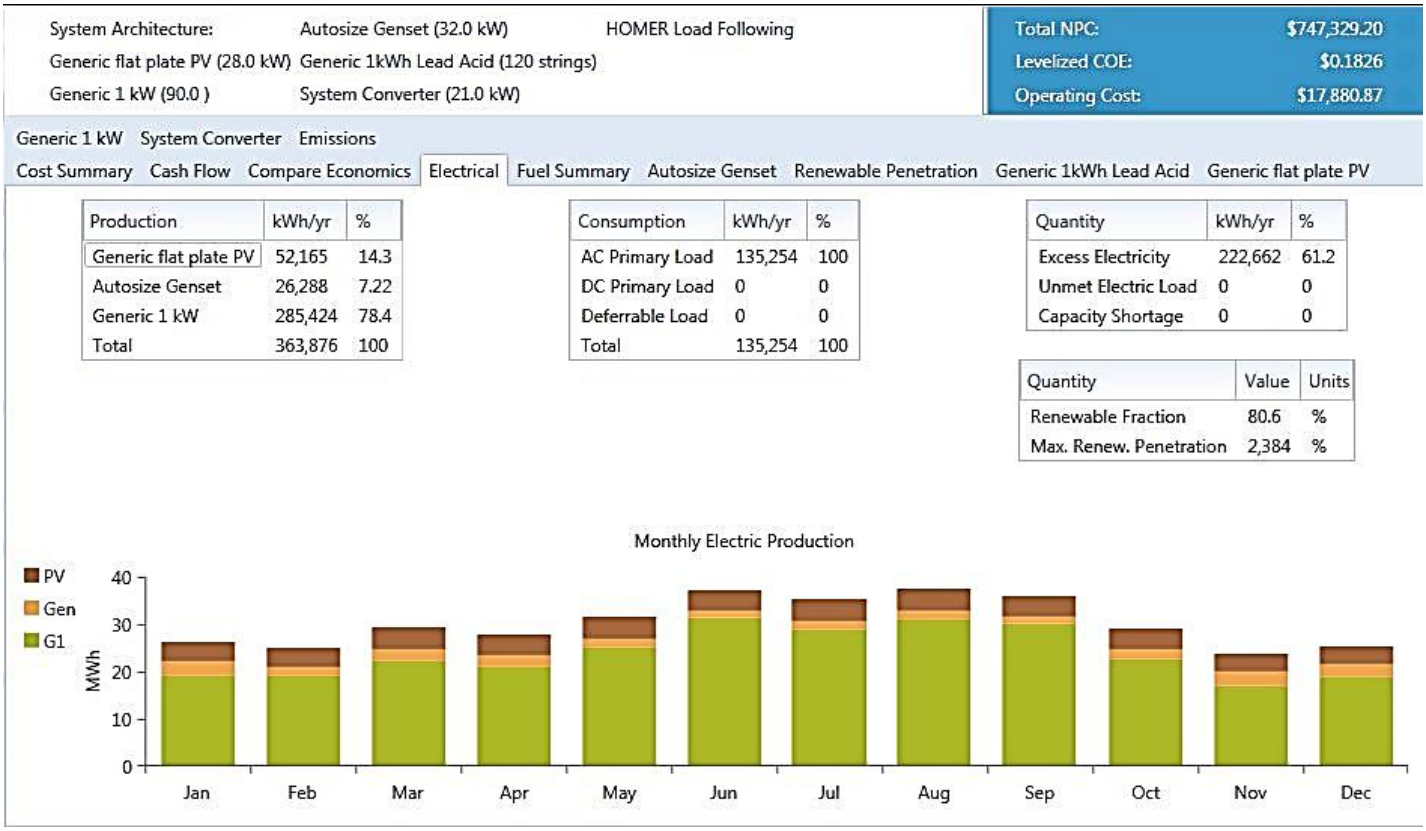

Fig. 17. Electrical Production Summary for HRES without DSM in Red Sea governorate

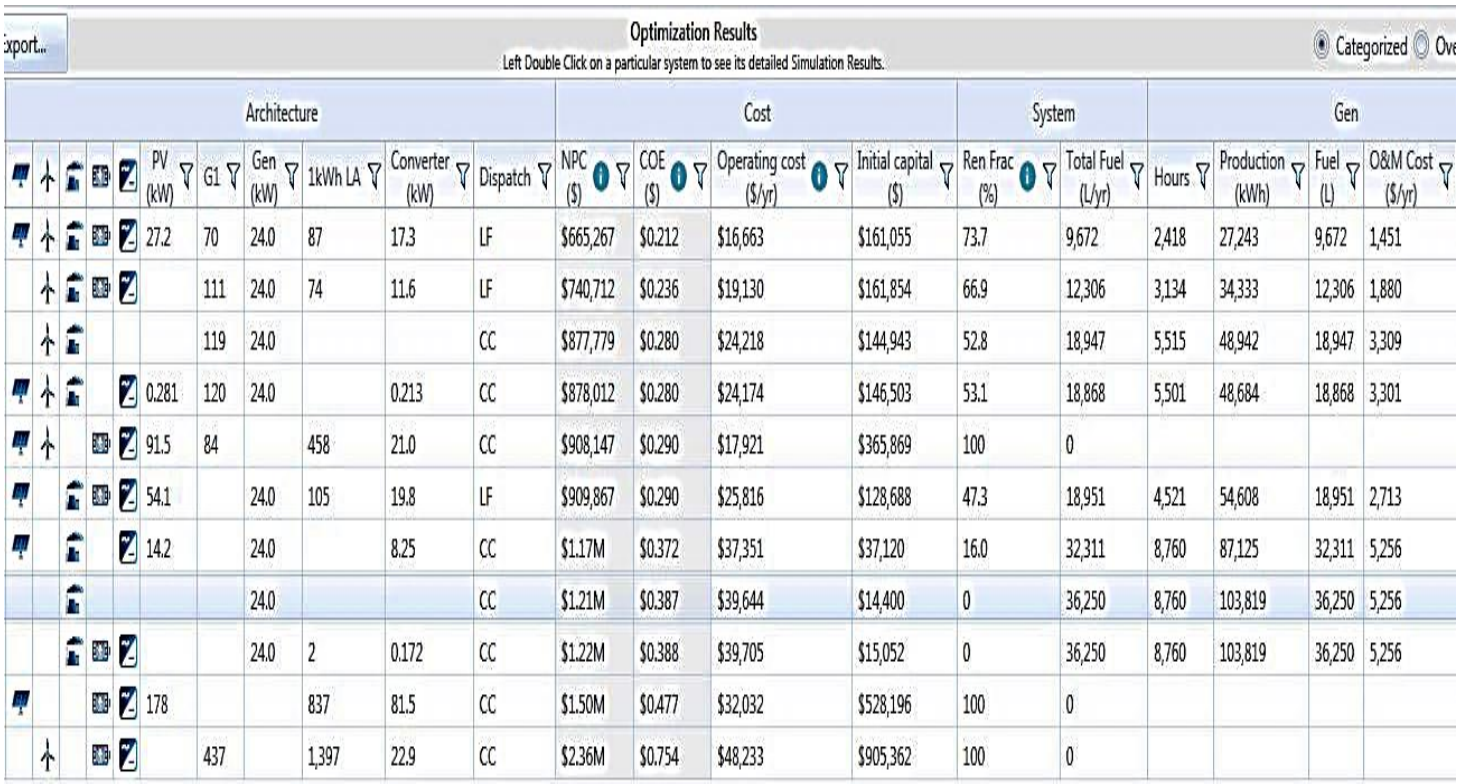

PV (kW)	G1	Gen (kW)	1kWh LA	Converter (kW)	Dispatch	NPC ($)	COE ($)	Operating cost ($/yr)	Initial capital ($)	Ren Frac (%)	Total Fuel (L/yr)	Hours	Production (kWh)	Fuel (L)	O&M Cost ($/yr)
27.2	70	24.0	87	17.3	LF	$665,267	$0.212	$16,663	$161,055	73.7	9,672	2,418	27,243	9,672	1,451
	111	24.0	74	11.6	LF	$740,712	$0.236	$19,130	$161,854	66.9	12,306	3,134	34,333	12,306	1,880
	119	24.0			CC	$877,779	$0.280	$24,218	$144,943	52.8	18,947	5,515	48,942	18,947	3,309
0.281	120	24.0		0.213	CC	$878,012	$0.280	$24,174	$146,503	53.1	18,868	5,501	48,684	18,868	3,301
91.5	84		458	21.0	CC	$908,147	$0.290	$17,921	$365,869	100	0				
54.1		24.0	105	19.8	LF	$909,867	$0.290	$25,816	$128,688	47.3	18,951	4,521	54,608	18,951	2,713
14.2		24.0		8.25	CC	$1.17M	$0.372	$37,351	$37,120	16.0	32,311	8,760	87,125	32,311	5,256
		24.0			CC	$1.21M	$0.387	$39,644	$14,400	0	36,250	8,760	103,819	36,250	5,256
		24.0	2	0.172	CC	$1.22M	$0.388	$39,705	$15,052	0	36,250	8,760	103,819	36,250	5,256
178			837	81.5	CC	$1.50M	$0.477	$32,032	$528,196	100	0				
	437		1,397	22.9	CC	$2.36M	$0.754	$48,233	$905,362	100	0				

Fig. 18. Optimization Results for HRES with DSM in Qena governorate

Export...

Optimization Results

Left Double Click on a particular system to see its detailed Simulation Results.

Categorized Overall

Architecture										Cost				System			Gen			
					PV (kW)	G1	Gen (kW)	1kWh LA	Converter (kW)	Dispatch	NPC ($)	COE ($)	Operating cost ($/yr)	Initial capital ($)	Ren Frac (%)	Total Fuel (L/yr)	CO_2 (kg/yr)	Hours	Production (kWh)	Fuel (L)	O&M Cost ($/yr)
✓	✓	✓	✓	✓	22.5	76	24.0	78	16.1	LF	$569,353	$0.181	$13,437	$162,743	80.7	7,137	18,682	1,804	19,990	7,137	1,082
	✓	✓	✓	✓		93	24.0	64	11.1	LF	$601,204	$0.192	$15,166	$142,270	74.3	9,589	25,099	2,465	26,621	9,589	1,479
	✓	✓				101	24.0			CC	$729,502	$0.232	$19,970	$125,197	61.8	15,541	40,681	4,613	39,636	15,541	2,768
✓	✓	✓		✓	0.120	94	24.0		0.131	CC	$731,129	$0.233	$20,270	$117,767	60.9	15,909	41,644	4,719	40,592	15,909	2,831
✓	✓		✓	✓	54.5	133		379	24.6	CC	$833,049	$0.266	$15,903	$351,841	100	0	0				
✓		✓	✓	✓	51.4		24.0	104	19.9	LF	$912,556	$0.291	$25,842	$130,573	47.4	18,940	49,577	4,514	54,600	18,940	2,708
	✓		✓	✓		315		413	29.6	CC	$1.07M	$0.340	$19,123	$487,237	100	0	0				
✓		✓		✓	14.3		24.0		7.56	CC	$1.17M	$0.373	$37,375	$39,182	16.0	32,302	84,553	8,760	87,087	32,302	5,256
		✓					24.0			CC	$1.21M	$0.387	$39,644	$14,400	0	36,250	94,888	8,760	103,819	36,250	5,256
		✓	✓	✓			24.0	2	0.172	CC	$1.22M	$0.388	$39,707	$15,103	0	36,250	94,888	8,760	103,819	36,250	5,256
✓			✓	✓	133			866	27.7	CC	$1.35M	$0.430	$29,201	$464,661	100	0	0				

Fig. 19. Optimization Results for HRES with DSM in Red Sea governorate

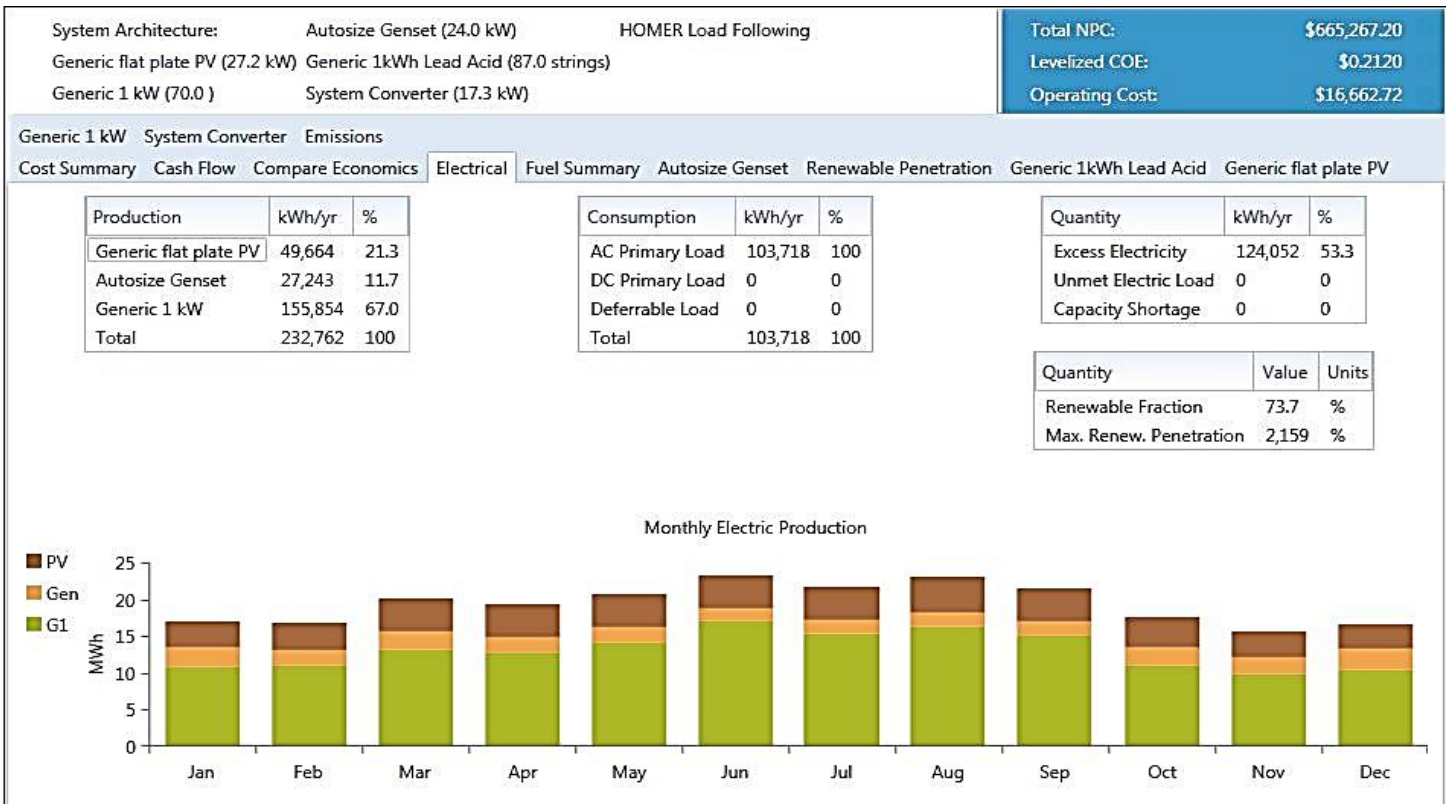

Fig.20. Electrical Production Summary for HRES with DSM in Qena governorate

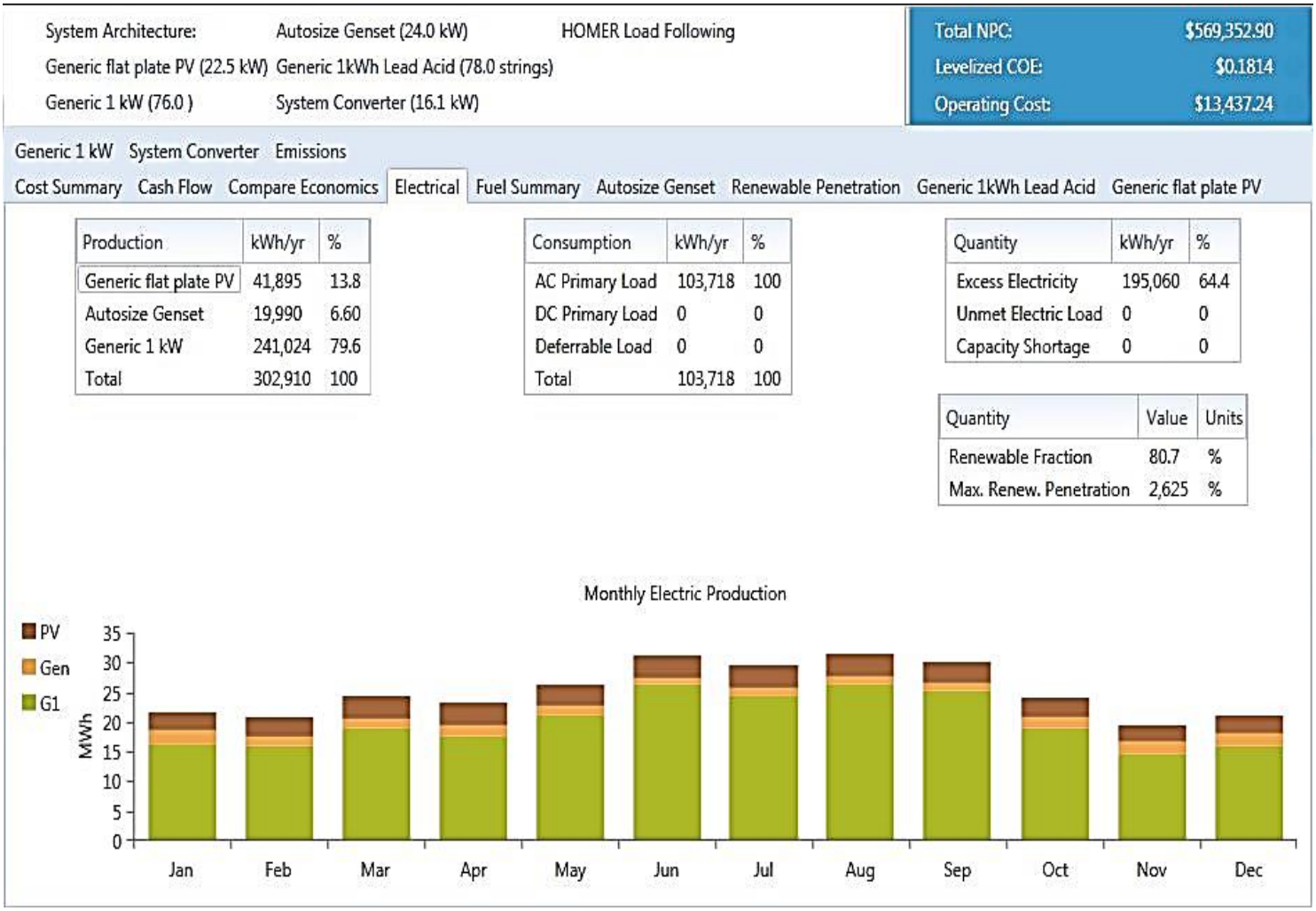

Fig. 21. Electrical Production Summary for HRES with DSM in Red Sea governorate

Table 6. Comparison between Three Systems in Qena governorate

Parameters		Energy-Economics		
		Diesel Power System (Base Case)	Hybrid System without DSM	Hybrid System with DSM
System Architecture	Generator (kW)	32	32	24
	PV (kW)	N/A	36.6	27.2
	Wind turbine (kW)	N/A	91	70
	Batteries (kWh)	N/A	115	87
	Bidirectional converter (kW)	N/A	23.4	17.3
Initial Capital Cost ($)		19,200	212,097	161,055

Operating Cost ($)	52,310	21,889	16,663
Total NPC ($)	1.60 M	874,443	665,267
Total Production (kWh/yr)	135,407	34,930	27,243
Unmet Electrical Load (kWh/yr)	0	0	0
COE ($/kWh)	0.391	0.214	0.212
Diesel Consumed	47,621	12,471	9,672
Renewable Fraction (%)	0	74.2	73.7

Table 7. Comparison between Three Systems in Red Sea governorate

Parameters		Energy-Economics		
		Diesel Power System (Base Case)	Hybrid System without DSM	Hybrid System with DSM
System Architecture	Generator (kW)	32	32	24.4
	PV (kW)	N/A	28	22.5
	Wind turbine (kW)	N/A	90	76
	Batteries (kWh)	N/A	120	78.
	Bidirectional converter (kW)	N/A	21	16.1
Initial Capital Cost ($)		19,200	206,256	162,743
Operating Cost ($)		52,310	17,881	13,437
Total NPC ($)		1.60 M	747,329	569,353
Total Production (kWh/yr)		135,407	26,288	19,990
Unmet Electrical Load (kWh/yr)		0	0	0
COE ($/kWh)		0.391	0.183	0.181
Diesel Consumed		47,621	9,405	7,137
Renewable Fraction (%)		0	80.6	80.7

References

[1] Y. Noorollahi, R. Itoi, H. Yousefi, M. Mohammadi, and A. Farhadi, "Modeling for diversifying electricity supply by maximizing renewable energy use in Ebino city southern Japan," *Sustainable cities and society,* vol. 34, pp. 371-384, 2017.

[2] S. Mandelli, J. Barbieri, R. Mereu, and E. Colombo, "Off-grid systems for rural electrification in developing countries: Definitions, classification and a comprehensive literature review," *Renewable and Sustainable Energy Reviews,* vol. 58, pp. 1621-1646, 2016.

[3] B. K. Sovacool and M. A. Brown, "Competing dimensions of energy security: an international perspective," *Annual Review of Environment & Resources,* vol. 35, pp. 77-108, 2010.

[4] M. Das, M. A. K. Singh, and A. Biswas, "Techno-economic optimization of an off-grid hybrid renewable energy system using metaheuristic optimization approaches–case of a radio transmitter station in India," *Energy conversion and management,* vol. 185, pp. 339-352, 2019.

[5] S. Sinha and S. Chandel, "Review of software tools for hybrid renewable energy systems," *Renewable and sustainable energy reviews,* vol. 32, pp. 192-205, 2014.

[6] B. Hartono, Y. Budiyanto, and R. Setiabudy, "Review of microgrid technology," in *2013 international conference on QiR*, 2013, pp. 127-132.

[7] P. Degobert, S. Kreuawan, and X. Guillaud, "Micro-grid powered by photovoltaic and micro turbine," in *International Conference on Renewable Energies in France*, 2006.

[8] M. Mohammadi, R. Ghasempour, F. R. Astaraei, E. Ahmadi, A. Aligholian, and A. Toopshekan, "Optimal planning of renewable energy resource for a residential house considering economic and reliability criteria," *International Journal of Electrical Power & Energy Systems,* vol. 96, pp. 261-273, 2018.

[9] J. Kartite and M. Cherkaoui, "Study of the different structures of hybrid systems in renewable energies: A review," *Energy Procedia,* vol. 157, pp. 323-330, 2019.

[10] B. Ye, P. Yang, J. Jiang, L. Miao, B. Shen, and J. Li, "Feasibility and economic analysis of a renewable energy powered special town in China," *Resources, Conservation and Recycling,* vol. 121, pp. 40-50, 2017.

[11] C. Li, D. Zhou, H. Wang, Y. Lu, and D. Li, "Techno-economic performance study of stand-alone wind/diesel/battery hybrid system with different battery technologies in the cold region of China," *Energy,* vol. 192, p. 116702, 2020.

[12] Z. Ding, H. Hou, G. Yu, E. Hu, L. Duan, and J. Zhao, "Performance analysis of a wind-solar hybrid power generation system," *Energy Conversion and Management,* vol. 181, pp. 223-234, 2019.

[13] A. Kaabeche, M. Belhamel, and R. Ibtiouen, "Sizing optimization of grid-independent hybrid photovoltaic/wind power generation system," *Energy,* vol. 36, pp. 1214-1222, 2011.

[14] R. Atia and N. Yamada, "Optimization of a PV-wind-diesel system using a hybrid genetic algorithm," in *2012 IEEE Electrical Power and Energy Conference*, 2012, pp. 80-85.

[15] M. K. Al-Saadi, P. C. Luk, and W. Fei, "Impact of unit commitment on the optimal operation of hybrid microgrids," in *2016 UKACC 11th International Conference on Control (CONTROL)*, 2016, pp. 1-6.

[16] H. Yang, L. Lu, and W. Zhou, "A novel optimization sizing model for hybrid solar-wind power generation system," *Solar energy,* vol. 81, pp. 76-84, 2007.

[17] A. K. Bansal, R. Gupta, and R. Kumar, "Optimization of hybrid PV/wind energy system using Meta Particle Swarm Optimization (MPSO)," in *India International Conference on Power Electronics 2010 (IICPE2010)*, 2011, pp. 1-7.

[18] F. Akram, F. Asghar, M. A. Majeed, W. Amjad, M. O. Manzoor, and A. Munir, "Techno-economic optimization analysis of stand-alone renewable energy system for remote areas," *Sustainable Energy Technologies and Assessments,* vol. 38, p. 100673, 2020.

[19] A. Nasser and P. Reji, "Optimal planning approach for a cost effective and reliable microgrid," in *2016 International Conference on Cogeneration, Small Power Plants and District Energy (ICUE)*, 2016, pp. 1-6.

[20] G. Tina, S. Gagliano, and S. Raiti, "Hybrid solar/wind power system probabilistic modelling for long-term performance assessment," *Solar energy,* vol. 80, pp. 578-588, 2006.

[21] A. Kaabeche, "Optimization of a completely autonomous hybrid system (wind photovoltaic)," *Rev mater énerg renouv,* vol. 9, 2006.

[22] L. Olatomiwa, S. Mekhilef, A. Huda, and O. S. Ohunakin, "Economic evaluation of hybrid energy systems for rural electrification in six geo-political zones of Nigeria," *Renewable Energy,* vol. 83, pp. 435-446, 2015.

[23] L. Bhamidi and S. Shanmugavelu, "Multi-objective harmony search algorithm for dynamic optimal power flow with demand side management," *Electric Power Components and Systems,* vol. 47, pp. 692-702, 2019.

[24] B. Lokeshgupta and S. Sivasubramani, "Multi-objective dynamic economic and emission dispatch with demand side management," *International Journal of Electrical Power & Energy Systems,* vol. 97, pp. 334-343, 2018.

[25] L. Bhamidi and S. Sivasubramani, "Optimal planning and operational strategy of a residential microgrid with demand side management," *IEEE Systems Journal,* vol. 14, pp. 2624-2632, 2019.

[26] J. Alqueres and J. Praca, "The Brazilian power system and the challenge of the Amazon transmission," in *Proceedings of the 1991 IEEE power engineering society transmission and distribution conference*, 1991, pp. 315-320.

[27] A. Willoughby, *Solar cell materials: developing technologies*: John Wiley & Sons, 2014.

[28] M. Kolhe, K. Agbossou, J. Hamelin, and T. Bose, "Analytical model for predicting the performance of photovoltaic array coupled with a wind turbine in a stand-alone renewable energy system based on hydrogen," *Renewable energy,* vol. 28, pp. 727-742, 2003.

[29] P. Gopi and I. P. Reddy, "Modelling and optimization of renewable energy integration in buildings," 2011.

[30] A. I. Iskanderani, I. M. Mehedi, M. A. Ramli, and M. Islam, "Analyzing the off-grid performance of the hybrid photovoltaic/diesel energy system for a peripheral village," *International Journal of Photoenergy,* vol. 2020, 2020.

[31] B. Guinot, B. Champel, F. Montignac, E. Lemaire, D. Vannucci, S. Sailler*, et al.*, "Techno-economic study of a PV-hydrogen-battery hybrid system for off-grid power supply: Impact of performances' ageing on optimal system sizing and competitiveness," *International journal of hydrogen energy,* vol. 40, pp. 623-632, 2015.

[32] M. R. Akhtari and M. Baneshi, "Techno-economic

assessment and optimization of a hybrid renewable co-supply of electricity, heat and hydrogen system to enhance performance by recovering excess electricity for a large energy consumer," *Energy Conversion and Management,* vol. 188, pp. 131-141, 2019.

[33] P. Morrone, A. Algieri, and T. Castiglione, "Hybridisation of biomass and concentrated solar power systems in transcritical organic Rankine cycles: A micro combined heat and power application," *Energy conversion and management,* vol. 180, pp. 757-768, 2019.

[34] J. Assaf and B. Shabani, "A novel hybrid renewable solar energy solution for continuous heat and power supply to standalone-alone applications with ultimate reliability and cost effectiveness," *Renewable Energy,* vol. 138, pp. 509-520, 2019.

[35] D. Wu and R. Wang, "Combined cooling, heating and power: A review," *progress in energy and combustion science,* vol. 32, pp. 459-495, 2006.

[36] H. Rezk, M. A. Abdelkareem, and C. Ghenai, "Performance evaluation and optimal design of stand-alone solar PV-battery system for irrigation in isolated regions: A case study in Al Minya (Egypt)," *Sustainable Energy Technologies and Assessments,* vol. 36, p. 100556, 2019.

[37] M. Hossain, S. Mekhilef, and L. Olatomiwa, "Performance evaluation of a stand-alone PV-wind-diesel-battery hybrid system feasible for a large resort center in South China Sea, Malaysia," *Sustainable cities and society,* vol. 28, pp. 358-366, 2017.

[38] M. O. Atallah, M. Farahat, M. E. Lotfy, and T. Senjyu, "Operation of conventional and unconventional energy sources to drive a reverse osmosis desalination plant in Sinai Peninsula, Egypt," *Renewable Energy,* vol. 145, pp. 141-152, 2020.

[39] M. Elkadeem, S. Wang, A. M. Azmy, E. G. Atiya, Z. Ullah, and S. W. Sharshir, "A systematic decision-making approach for planning and assessment of hybrid renewable energy-based microgrid with techno-economic optimization: A case study on an urban community in Egypt," *Sustainable Cities and Society,* vol. 54, p. 102013, 2020.

[40] H. Rezk, E. T. Sayed, M. Al-Dhaifallah, M. Obaid, M. Abou Hashema, M. A. Abdelkareem*, et al.*, "Fuel cell as an effective energy storage in reverse osmosis desalination plant powered by photovoltaic system," *Energy,* vol. 175, pp. 423-433, 2019.

[41] M. Seifi, A. C. Soh, M. K. Hassan, and N. I. A. Wahab, "An innovative demand side management for vulnerable hybrid microgrid," in *2014 IEEE Innovative Smart Grid Technologies-Asia (ISGT ASIA)*, 2014, pp. 797-802.